Rydberg-atom simulator and quantum many-body scars

Michelle Wu
Department of Physics, Stanford University, Stanford, CA 94305
(Dated: June 27, 2020)

Submitted as coursework for PH470, Stanford University, Spring 2020

Physicists have been working on engineering quantum materials in order to build highly tunable, coherent quantum simulators that serve as a tool to solve problems in many-body physics that require heavy numerical calculation and also a candidate to the realization of quantum computers. In this paper, I will review the realization of Rydberg-atom simulator and how it leads us to quantum many-body scars.

©*(Michelle Wu). The author warrants that the work is the author's own and that Stanford University provided no input other than typesetting and referencing guidelines. The author grants permission to copy, distribute, and display this work in unaltered form, with attribution to the author, for noncommercial purposes only. All of the rights, including commercial rights, are reserved to the author.*

I. INTRODUCTION

A fully controlled, coherent many-body quantum system is an ideal system for quantum simulation. Such systems shade light on research regarding strongly correlated quantum systems, quantum entanglement, new states of matter, and quantum information processors.[1] Quantum simulation and computation have been studied in a variety kind of platforms, such as trapped ions[2] and superconducting qubits[3]. Using neutral atoms as a platform has several advantages: 1. such systems have coherent properties, 2. it is easy to create a large number of atoms, 3. atoms can be strongly coupled to light. However, the disadvantages include the weak interaction between atoms and the challenge to control neutral atoms individually.

The Lukin group (Bernien et. al.) from Harvard University realized a 51-qubits quantum simulator using Rydberg atoms array[4] that circumvents those problems. Making use of the long lifetime and strong interaction of Rydberg atoms with clever trapping skills, they are able to create a quantum material system that simulate Ising-type quantum spin model. They observe different phases of ordered states that break various discrete symmetries. Also, although this system is not integrable, they observe exotic many-body dynamics that seem to be non-ergodic. This hints the observation of quantum many-body scar. After their publication, Turner et. al. from University of Leeds published a theoretical paper using the same system as the experimental work done by the Lukin group but using L = 32 as the system size instead. They further interpret the experimental observation as a result of weak ergodicity breaking due to the special eigenstates in the spectrum. This resembles quantum scars in chaotic non-interacting systems.[5]

In this paper, I will first review the experimental work done by the Lukin group and then show how Turner et. al. come to the conclusion that the observed exotic behavior is a realization of quantum scar.

II. EXPERIMENTAL OBSERVATION

A. Rydberg atoms and Rydberg blockade

Rydberg atoms are atoms being in the excited states with a large quantum number, n. Such excited states are called Rydberg state. In Rydberg states, n is so large that the electron is only weakly bound to the ionic core, making it sensitive to external electric field. The polarizability $\alpha \sim n^7$. The same also applies when the electric field is generated by the charge distribution of another Rydberg atom. Thus, Rydberg atoms exhibits very strong interactions. The large quantum number also gives Rydberg atoms long lifetimes since the lifetime $\tau \sim n^3$ if directly decay to ground state and $\tau \sim n^5$ if decaying through other Rydberg states.

The interaction between Ryderbeg atom pairs is van der Waals interaction and it scales as $\sim n^{11}/r^6$, where r is the distance between the atoms. When bringing two atoms too close together, the dipole-dipole interation between two atoms shifts the Rydberg level of one atom far away from resonance, making it unable to be excited. We say that this atom is blocked. This phenomenon that we can only excite one atom is called Rydberg blockade. It has been used to generate quantum gates[6] To observe Rydberg blockade, two conditions have to be fulfill: 1. atoms should be close enough to have strong interaction. 2. Atoms should be far enough that they can be individually controlled. Therefore, the Lukin group uses tightly focused laser traps, the so-called optical tweezer arrays, to explicitly control those atoms.

B. Rydberg atom array as a quantum simulator

The quantum dynamic of Rydberg atom array can be described by the Hamiltonian

$$H = \sum_i \frac{\Omega_i}{2} X_i - \sum_i \Delta_i n_i + \sum_{i<j} V_{ij} n_i n_j \qquad (1)$$

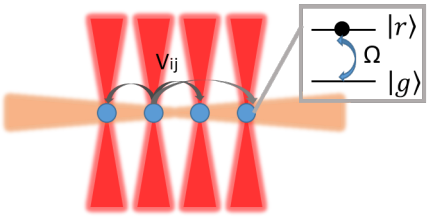

FIG. 1: Rydberg atoms(blue) are trapped individually inside tweezer arrays(red) and coupled by Rydberg lasers(orange).

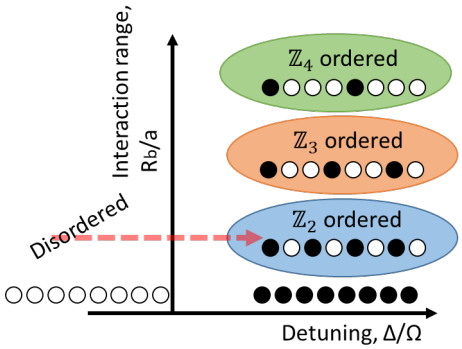

FIG. 2: A schematic phase diagram of the Hamiltonian in equation (1). The white circle represents ground state, and the black circle represents Rydberg state. Figure adapted from Bernien et al.[4]

assuming $\hbar = 1$. Δ_i are the detunings of the driving lasers from the Rydberg state, $X_i = \sigma_x^i = |g_i\rangle\langle r_i| + |r_i\rangle\langle g_i|$ is the Pauli X operator. It describes the coupling between the ground state $|g_i\rangle$ and the Rydberg state $|r_i\rangle$ of an atom at position i. $n_i = |r_i\rangle\langle r_i|$, and Ω_i is the Rabi frequency of the system. This paper focus on the homogeneous coherent coupling, the condition that $|\Omega_i| = \Omega, \Delta_i = \Delta$. These two parameters can be controlled by changing laser intensities and detunings in time. The Rydberg-Rydberg interation V_{ij} can be tuned by changing the distance between atoms or by coupling atoms to a different Rydberg state.

The experimental protocol that Lukin group implements is as follows: The cold atoms are first loaded from a magneto-optical trap to tightly focused laser trap array, as shown in Fig. 1 To remove the entropy from the system, they simply take a fluorescence image of the system to identify the position of the empty tweezers and then remove those traps. The remaining traps are then rearranged and form a regular atom array. Next, the traps are turned off and the system evolve under the unitary time evolution $U(\Omega, \Delta, t)$. This is realized by coupling the atoms to the Rydberg state $|r\rangle = |70S_{1/2}\rangle$

One constraint that should be considered here is Rydberg blockade. It happens when two atoms are close enough that $V_{ij} > \Omega$. When $V_{ij} = \Omega$, we define the Rydberg blockade radius R_b. Here, $R_b = 9\mu m$. Rydberg blockade can be generalized to multi-atom situation, that is, if we have multiple atoms within Rydberg radius, we would only be able to excite one of them. The system would only have two effective states, ground state being $|g_1 g_2 g_3 ....\rangle$, where all atoms are in $|g\rangle$, and the excited state being $1/\sqrt{N}(\sum_i |g_1 ... r_i ... g_N\rangle)$. This is a superposition of the states where only one atom is excited and others remain in the ground state, assuming we have N atoms.

The Hamiltonian for this system resembles the Ising-type spin model. By tuning the detuning, Δ/Ω and the interaction range R_b/a, where a being the trap spacing, different phases can be presented, as illustrated in Fig. 2. For example, at large negative values of Δ/Ω, the system will be in its ground state, where all the atoms are in the state $|g\rangle$. As we increase Δ/Ω toward positive value, the number of atoms in $|r\rangle$ increases. In this region, the interaction range become important because Rydberg blockade needs to be considered. By tuning the interaction range, we can create situations such as $V_{i,i+1} \gg \Delta \gg \Omega \gg V_{i,i+2}$. This is the case that blockade happens for neighbouring atoms. In this case, the atom array will arrange like $|r_1 g_2 r_3 g_4 ...\rangle$. $\mathbb{Z}_2$ translational symmetry is broken and we call this state $\mathbb{Z}_2$-ordered states. In the situation that $V_{i,i+1}, V_{i,i+2} \gg \Delta \gg \Omega \gg V_{i,i+3}$, blockade happens for every three nearest atoms. This results in states such as $|r_1 g_2 g_3 r_4 g_5 g_6 ...\rangle$. This is the $\mathbb{Z}_3$-ordered state. By extending blockade, $\mathbb{Z}_n$-ordered states can be created. In the experiment, they first prepare the initial state in $|g_1 g_2 g_3 ....\rangle$ by optical pumping and let the laser detuning $\Delta < 0$. They then adiabatically sweep the detuning to positive to reach one of the $\mathbb{Z}_n$-ordered states. By varying the trap spacing a, the distance between atoms in the array is changed, resulting in different phases (different symmetry breaking).

C. Quench dynamics

Beside adiabatic sweep in $\mathbb{Z}_n$-ordered states, Lukin group also presents the quench dynamics in the $\mathbb{Z}_2$-ordered phase. Starting from the $\mathbb{Z}_2$-ordered state, they suddenly change the detuning to resonance $\Delta = 0$. After this quench, they observe coherent and persistent oscillations as shown in Fig. 3. The oscillation persist beyond $1/\Omega$ and $1/V_{i,i+1}$. This is surprising because the persistent oscillations hint a non-ergodic, thus ETH breaking behavior, however, the only known conserved quantity of the Hamiltonian is the total energy, meaning that this system is not an integrable system. This behavior is not likely to be dependent of the system size since the array of 9 atoms and 51 atoms have a similar behavior after the quench. This is shown in Fig. 4 With the help of numerical calculation, they conclude that the decay of the oscillation is controlled by the next-nearest-neighbor interaction.

In addition, they compare the oscillation behavior of the $\mathbb{Z}_2$-ordered state and the state $|g_1 g_2 g_3 ...\rangle$ after a

quench. The initial state $|g_1 g_2 g_3 ....\rangle$ Hamiltonian quickly reach thermal equilibrium compared to the $\mathbb{Z}_2$-ordered state case. The interpretation of this persistent oscillation described above hinting the dynamic that the system neither obey ETH nor strongly break ETH remain unclear.

III. THEORETICAL MODEL

A. Thermalization and quantum scar

Thermalization in classical mechanics is based on the ergodic hypothesis. If, after a long period of time, all microstates of the system are accessed with equal probability, the system reaches thermal equilibrium. In quantum mechanics, however, this definition cannot be directly translated since the probability of finding the system in a given state is based on the choice of the initial state, making one unable to track a trajectory in the phase space. Therefore, the eigenstate thermalization hypothesis (ETH)[7], describing thermalization in isolated quantum systems using properties of eigenstates, is proposed. Isolated quantum systems that present ergodic dynamics are systems that obey ETH and are regarded as being able to reach thermal equilibrium.

The highly non-equilibrium quantum matter has been realized in a variety of platforms such as ultracold atoms, trapped ions, and nitrogen-vacancy in diamond. Those systems such as integrable systems and many-body localized systems strongly violate ETH. This motivates the question that whether systems that only weakly violate ETH exist?

Turner et. al. provide a theoretical model based on the dynamic of Rydberg atom array described in the previous section and claim that this is a system that weakly violate ETH[5]. The distinct behavior of this system is called "quantum many-body scarring."

B. PXP model

Note that the n_i in equation (1) corresponds to the density of excitations on site i and $n_i = (1 + Z_i)/2$, whereX_i, Y_i, Z_i are Pauli operators. Consider the limit situation that nearest-neighbor interaction $V_{i,i+1} \gg \Delta, \Omega$. Assuming $\Delta = 0, v = V_{i,i+1}$ and rescale the Hamiltonian in equation (1) by 1/V, we have

$$H' = H_0 + \epsilon H_1 = \sum_i n_i n_{i+1} + \epsilon \sum_i X_i \qquad (2)$$

, where $\epsilon = \Omega/2V$ is a small perturbation. Under the constraint of Rydberg blockade, it is useful to introduce the projector $P_i = |g_i\rangle\langle g_i| = (1 - Z_i)/2$.

The effective Hamiltonian can be obtained by the Schrieffer-Wolff transformation. We are interested in the low-energy subspace that no adjacent excited states exist. The projector onto this subspace is $P = \prod_i (1 - n_i n_{i+1})$. In this subspace, H_0 in equation (2) vanishes so the first non-trivial order would be $H_{SW} = \epsilon P H_1 P$. Rescaling again, the Hamiltonian can be written as

$$H = \sum_i P_{i-1} X_i P_{i+1} \qquad (3)$$

This is the so-called PXP model. P_i here makes sure that only one of the two adjacent atoms can be in excited state. This constraint comes from Rydberg blockade. For spins-1/2 chain, the Hilbert space dimension D scales as 2^L, where L is the system size. Now that adding an additional atom to the chain increases the dimension by an amount smaller than the spin-1/2 chain case adjacent excitation is not allowed. Under this constraint, D scales as $F_{L+1} + F_{L-1}$, where F_n is the nth Fibonacci number. Here we consider periodic boundary conditions (PBC).

Inspired by the experiment performed by the Lukin group, the Turner group starts by considering the initial state $|g_1 g_2 g_3 ...\rangle$ and the $\mathbb{Z}_k$-ordered states, which means that atoms in excited states are separated by $k-1$ atoms in the ground state. Using infinite time evolving block decimation (iTEBD) method, they found that the entanglement entropy for the midpoint bipartition for all initial states mentioned before grow linearly, as shown in Fig. 5 The slope however, depends on the initial state. The $\mathbb{Z}_2$-ordered state has the smallest slope. Besides linear growth, weak oscillations are also observed. By subtracting the linear component, the period of oscillations is 2.35, which are found to be the same as the experimental observation.[4] This is remarkable because the state $|g_1 g_2 g_3 ...\rangle$ and the $\mathbb{Z}_2$-ordered states has the same energy under the Hamiltonian described in equation (2). Thus we expect them to reach the same temperature if the system thermalizes. However, the $\mathbb{Z}_2$-ordered state shows oscillations and does not thermalize for a long time.

C. Special eigenstates

In this section I will show how the Turner group reaches a conclusion that the observed oscillations are due to the existence of special eigenstates.

If a system reaches thermal equilibrium, the initial state and the eigenstates should be independent with each other. To research on the thermalization of this system, the Turner group first try to look at the overlap between the initial state of the system, the $\mathbb{Z}_2$-ordered state, and the eigenstates of the Hamiltonian in equation (3) as shown in Fig. 6 The exact eigenstates are obtained under the condition that system size L = 32 and PBC. We can see that there is a "band" of eigenstates that are highly overlap with the $\mathbb{Z}_2$-ordered state. Moreover, the energy spacing between these states stay constant and it agree with the oscillation frequency obtained by iTEBD method, for up to a factor of 2. This factor of 2 comes from the indistinguishable of $|\mathbb{Z}_2\rangle = |grgr...\rangle$ and $|\mathbb{Z}_2'\rangle = |rgrg...\rangle$. The Tuner group then characterize these

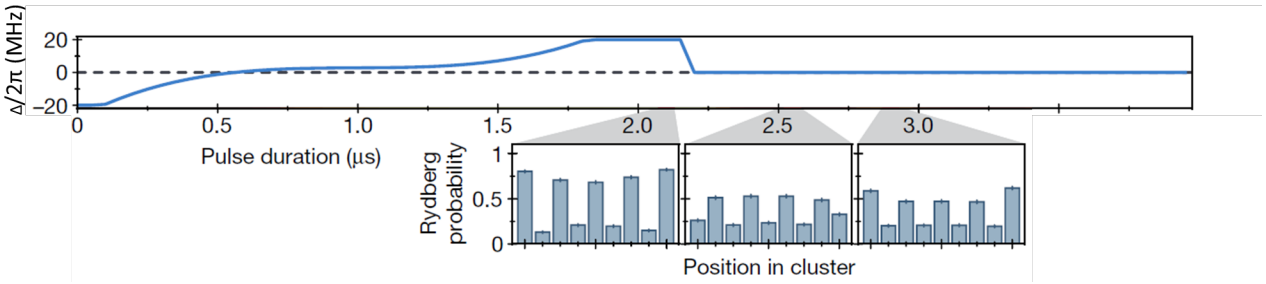

FIG. 3: Oscillation observed after sudden quench. This data is taken from a cluster of 9 atoms. The initial cluster is at time $t \sim 2$ when the detuning Δ is tuned to zero, this configuration that the Rydberg excitation being at every odd trap site collapsed to a configuration that the excitation being at every even trap site at $t \sim 2.5$ and revive later at $t \sim 3$. Figure adapted from Bernien et al.[4]

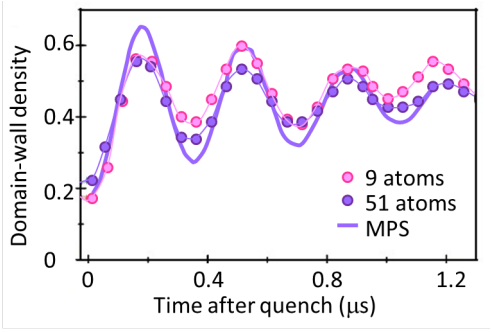

FIG. 4: Similar persistent oscillations behavior for different system sizes. Solid purple line is a fully coherent matrix product state (MPS) simulation with bond dimension D = 256. Figure adapted from Bernien et al.[4]

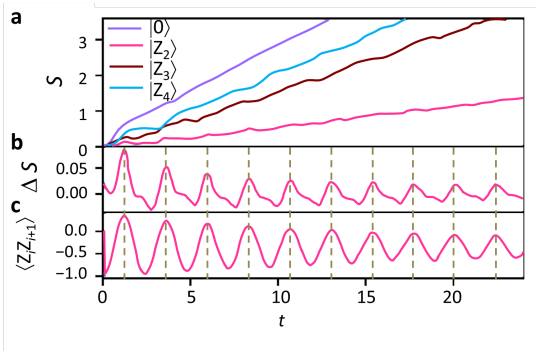

FIG. 5: (a) Entanglement entropy for different initial states. (b), (c) For the $|\mathbb{Z}_2\rangle$ initial state the entanglement entropy oscillates around the linear growth with the same frequency as the local correlation functions. The period of the oscillation is found to be the same as the experimental observation from the Lukin group. Figure adapted from Turner et al.[5]

special eigenstates by forward scattering approximation (FSA) method.

To compare the difference of two states, we introduce Hamming distance, which means The number of different sites between two states. For example, the Hamming distance between $|ggg\rangle$ and $|rrg\rangle$ is two. The Hamiltonian can be splitted as $H = H^+ + H^-$, where

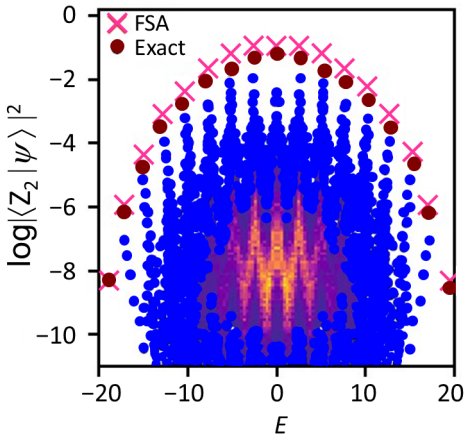

FIG. 6: Scatter plot of the overlap of many-body eigenstates of the Hamiltonian in equation (3) and the $\mathbb{Z}_2$ product state. This shows a band of special eigenstates separated from the remaining eigenstates. Crosses denote overlaps with eigenstates from the FSA approximation. The density of data points (shown in the middle of the graph) illustrates the tower structure in the overlaps. Figure adapted from Turner et al.[5]

$$H^+ = \sum_{i\in even} P_{i-1}\sigma_i^+ P_{i+1} + \sum_{i\in odd} P_{i-1}\sigma_i^- P_{i+1} \qquad (4)$$

$\sigma_i^+ = |r_i\rangle\langle g_i|$ and $\sigma_i^- = |g_i\rangle\langle r_i|$. H^+ acting on $|\mathbb{Z}_2\rangle$ gives a single spin flip and increases the Hamming distance by one. H^- decreases the Hamming distance. Starting form the initial state $|0\rangle = |\mathbb{Z}_2\rangle$ and going forward by acting H^+ on the states, a basis $\{|n\rangle\}$ can be obtained. $|n\rangle = (H^+)^n|\mathbb{Z}_2\rangle / \| (H^+)^n |\mathbb{Z}_2\rangle | \|$. This structure enable us to write the Hamiltonian in a tri-diagonal martrix form

$$H_{FSA} = \begin{pmatrix} 0 & \beta_1 & & & \\ \beta_1 & 0 & \beta_2 & & \\ & \beta_2 & 0 & \ddots & \\ & & \ddots & \ddots & \beta_L \\ & & & \beta_L & 0 \end{pmatrix} \quad (5)$$

, where $\beta_n = \langle n+1|H^+|n\rangle = \langle n|H^-|n+1\rangle$. Turner et al. compare H_{FSA} with the special "band" described before and find that they are highly overlapped as shown in Fig. 6. More specifically, they find that FSA approximation agrees very will with the lowest-energy special states. Though the approximation overestimates for the states in the middle of the band, it captures the oscillation. (Further data can be found in the paper[5]) The FSA basis states form an orthogonal subspace $\{|n\rangle\}$ of dimension L + 1 and the scarred eigenstates can be compactly represented as linear superpositions of L + 1 of those basis states.

It is surprising that the FSA is able to successfully predict the exact eigenstates since the FSA basis has only L + 1 states and each of them concentrated in small parts of the Hilbert space. For a highly excited eigenstate of a thermalizing system of size L, this would provide a poor approximation. This further reveals the atypical nature of the special eigenstates.

IV. DISCUSSION

Though the cause of quantum scar are still not well understood, the surprising long-lived, periodic revivals after quantum quenches in Rydberg atom arrays performed by Bernien et al. and the theoretical model, especially the PXP model that suggests quantuam scars proposed by Turner et al. have drawn a lot of further discussions.[8][9][10] Similar scarring behavior has also been observed in a 1d dipoler gas.[11]

Because of the coherent property and being able to "memorize" the initial states, quantum scaring seems to be a potential way to protect qubits from outside disturbances that lead to information loss. Besides thermalizing problems in many-body physics, the research in quantum scar also open new possibilities to quantum computing.

[1] Ladd, T. D. et al. Quantum computers. Nature 464, 45–53 (2010).

[2] Gärttner, M. et al. Measuring out-of-time-order correlations and multiple quantum spectra in a trapped-ion quantum magnet. Nat. Phys. 13, 781–786 (2017).

[3] Song, C. et al. 10-qubit entanglement and parallel logic operations with a superconducting circuit. Phys. Rev. Lett. 119, 180511 (2017).

[4] Bernien et al., Probing many-body dynamics on a 51-atom quantum simulator, Nature 551, 579-584 (2017)

[5] Turner et al., Quantum many-body scars, Nature Physics (2018)

[6] Jaksch, D. et al. Fast quantum gates for neutral atoms. Phys. Rev. Lett. 85, 2208–2211 (2000).

[7] Srednicki, The approach to thermal equilibrium in quantized chaotic systems, J. Phys. A 32 (1999) 1163

[8] Turner et al., Quantum scarred eigenstates in a Rydberg atom chain: Entanglement, breakdown of thermalization, and stability to perturbations, Phys. Rev. B 98, 155134 (2018).

[9] Khemani, Vedika et al. Signatures of integrability in the dynamics of Rydberg-blockaded chains, Phys. Rev. B 99, 161101(R) (2019).

[10] Ho, Wen Wei et al. Periodic Orbits, Entanglement, and Quantum Many-Body Scars in Constrained Models: Matrix Product State Approach, Phys. Rev. Lett. 122, 040603 (2019).

[11] Kao, Wil et al. Creating quantum many-body scars through topological pumping of a 1D dipolar gas, arxiv.org/abs/2002.10475